JTTEE5 11:496-507

Cold Spray Nozzle Mach Number Limitation

B. Jodoin

(Submitted 14 February 2001; in revised form 11 June 2001)

The classic one-dimensional isentropic flow approach is used along with a two-dimensional axisymmetric numerical model to show that the exit Mach number of a cold spray nozzle should be limited due to two factors. To show this, the two-dimensional model is validated with experimental data. Although both models show that the stagnation temperature is an important limiting factor, the one-dimensional approach fails to show how important the shock-particle interactions are at limiting the nozzle Mach number. It is concluded that for an air nozzle spraying solid powder particles, the nozzle Mach number should be set between 1.5 and 3 to limit the negative effects of the high stagnation temperature and of the shock-particle interactions.

Keywords cold spray, numerical modeling, shock-particle interaction, supersonic flow

1. Introduction

Cold gas dynamic spray (CGDS) processing is a fairly new material process that has been developed in the 1980s at the Institute of Theoretical and Applied Mechanics of the Siberian Division of the Russian Academy of Science in Novosibirsk.[1,2] As opposed to other spray processes like thermal plasma spraying or high velocity oxygen fuel (HVOF) spraying, the cold spray process does not involve a major heating of the fluid and powder particles. Instead, the powder particles are accelerated above a critical velocity by a supersonic flow through momentum transfer. Once above this critical velocity, the particles impact on a substrate and deform plastically to form the coating, without having been melted. The deposition efficiency of the CGDS process increases with the powder particles velocity, and it has been found that for many materials the critical velocity is above 700 m/s,[3] explaining the need for the supersonic carrier flow. Many materials have been successfully sprayed so far, including a wide range of pure metals, polymers, and composites. Among all the benefits of the cold spray process, the major one is that the material to be sprayed is not heated to temperatures at which any significant chemical changes can be observed. The grain structure of the coating remains of the same order as the initial powder, a noticeable advantage over the other spraying methods.

An extensive analytical study of the nozzle geometry, based on the one-dimensional flow model,[4] has been performed to determine the optimal nozzle shape given the gas conditions, powder properties, and nozzle length.[5] It was shown that the spray particle velocity is relatively insensitive to the nozzle shape and therefore that a single nozzle can be used for a variety of operational conditions, as long as no shock waves are present in the nozzle. It has been shown experimentally that the deposition efficiency drops rapidly when copper (Cu) powder particles are decelerated below 600 m/s.[6] It was also shown that large Cu particles (22 μm diameter) do not suffer from considerable velocity reduction as they get close to the stagnation point on the substrate.[6] However, as the technology evolves, the use of smaller powder particles is envisioned, and it was found experimentally that Cu powder particles 5 μm in diameter or less are considerably slowed down in the vicinity of the substrate when the jet Mach number was fixed at 3.2.[2] This, in turn, reduces the spraying efficiency considerably.

In the design phase of a cold spray nozzle, the particle velocity required for the particles to bond correctly to the substrate is known. Therefore, the minimum nozzle exit gas velocity is provided by that value. The gas density and the length of the nozzle determine primarily how close the particles come to the gas velocity,[5] and an exit gas velocity above the critical velocity is usually used. At this speed, the flow is usually supersonic. How-

B. Jodoin, Assistant Professor, Mechanical Engineering, Faculty of Engineering, University of Ottawa, 770 King-Edward Ave., P.O. Box 450, Stn. A, Ottawa, Ontario K1N 6N5 Canada. Contact e-mail: jodoin@genie.uottawa.ca.

Nomenclature

A^*	nozzle throat area, m^2
A_e	nozzle exit plane area, m^2
C	speed of sound, m/s
C_D	drag coefficient, 1
C_p	constant pressure specific heat, J/kg · K
C_v	constant volume specific heat, J/kg · K
D	drag force, N
dt	time step, s
M	gas Mach number, 1
m	mass of a solid particle, kg
P_0	stagnation pressure, Pa
P_b	chamber back pressure, Pa
R	specific gas constant, J/kg · K
r_{part}	radius of a solid particle, m
T_0	stagnation of temperature, K
T_e	exit gas temperature, K
V	velocity, m/s
$V_{critical}$	critical velocity, m/s
V_{rel}	relative velocity between the gas and particle, m/s
X	position, m
γ	specific heat ratio, 1
ρ	mass density, kg/m^3
ρ_{part}	mass density of a solid particle, kg/m^3

ever, there are many possible design Mach numbers that can be used to obtain the desired gas velocity. This paper will look at two factors that may limit the nozzle design Mach number, namely, the stagnation temperature and the shock wave-particle interactions.

The paper is organized as follows. In Section 2, a brief overview of the technique used to generate a supersonic flow in the CGDS process is conducted to show that the stagnation temperature does not play any role in the nozzle exit Mach number determination. Section 3 follows with the development of the two factors limiting the design exit Mach number using the one-dimensional isentropic flow analysis. Sections 4 and 5 present the experimental procedure used to validate a two-dimensional axisymmetric model along with three validation test cases. Section 6 presents the results obtained from the two-dimensional axisymmetric model and gives the Mach number limitations. Finally, Section 7 concludes the findings of the paper.

2. Supersonic Flow Generation in CGDS: One-Dimensional Isentropic Flow Approach

In this section, the one-dimensional isentropic flow analysis is used to show the general and specific nozzle geometry and pressure ratio required to generate a shock-free supersonic flow. Only the main results of this analysis are presented here. Readers should refer to Compressible Fluid Mechanics textbooks for more details.[4] The one-dimensional isentropic analysis is restrictive due to the assumptions it uses. However, it shows that the nozzle geometry and the pressure ratio are the only factors to consider when designing a CGDS nozzle operating at a specific Mach number. The equations presented in this section will be used in the next section to show that the stagnation temperature does not play any role in the flow exit Mach number.

2.1 General Geometry Requirement

Historically, one-dimensional isentropic flow analysis has been used to show how to generate a supersonic flow. This analysis assumes that the flow inside a variable area duct is one-dimensional, in steady-state, and that there is no chemical reaction, no external work done on the flow, no change in the potential energy, no heat transfer occurring, and the flow is reversible. Under these assumptions the mass conservation, energy conservation, and second law of thermodynamics show that the general geometry required to accelerate a subsonic flow to the supersonic regimen is a convergent-divergent nozzle.[4] With this geometry, the fluid is continuously accelerated from low subsonic to supersonic velocity. The flow passes through the sonic condition ($M = 1$) at the junction of the converging and the diverging parts, called the throat. Another requirement must also be fulfilled to create a supersonic flow: the pressure ratio between the stagnation pressure of the flow and the back pressure outside the nozzle.

2.2 Pressure Ratio for a Shock-Free Supersonic Nozzle Flow

It is not sufficient to use a convergent-divergent nozzle to obtain a supersonic flow. The proper gas stagnation pressure must also be used to ensure a supersonic flow at the nozzle exit. Figure 1 is used to illustrate that concept.

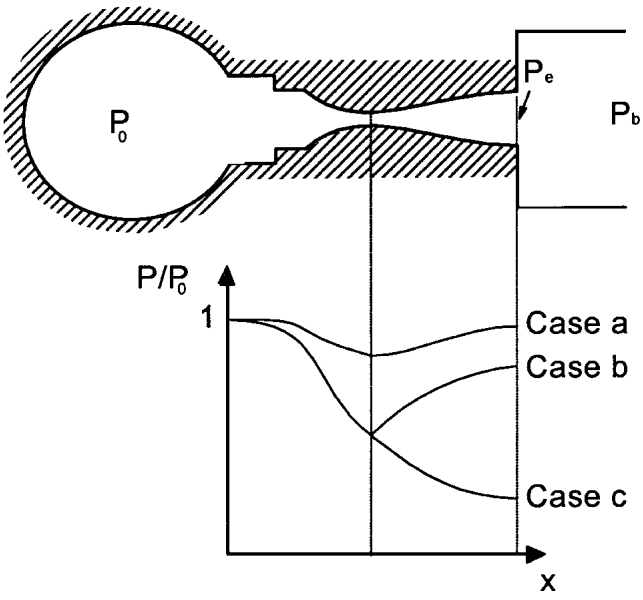

Fig. 1 Pressure distribution in the nozzle for three back pressures (P_b). Case **(a):** The flow is subsonic everywhere. Case **(b):** The flow is subsonic everywhere, except at the throat where it is sonic. Case **(c):** The flow is subsonic in the convergent and supersonic in the divergent. A shock wave will be present in the nozzle or in the free jet if the back pressure is set at a value between Case (b) and Case (c). Shock waves will be present in the free jet if the back pressure is set at values below the pressure of Case (c).

It illustrates a large gas reservoir connected to a convergent-divergent nozzle discharging in a controlled pressure chamber. All the assumptions stated in the previous section are used. The properties of the fluid in the reservoir are kept constant and are the stagnation properties of the fluid. P_0 is the stagnation pressure of the fluid in the reservoir, P_e is the fluid pressure at the exit plane of the nozzle, and P_b is the controlled chamber back pressure. Three cases of pressure ratio P_b/P_0 are presented to illustrate the behavior of the flow.

In Case (a), P_b is slightly lower than P_0. The gas accelerates in the convergent where the pressure decreases. The throat Mach number is less than 1, so the flow is subsonic when it reaches the divergent. The flow decelerates in the divergent where P_e rises back to the level of P_b. The flow at the nozzle exit is subsonic. In Case (b), P_b is low enough that the Mach number reaches 1 at the throat. However, the flow returns to subsonic velocities in the divergent because P_e has to rise back to P_b at the exit. In Case (c), P_b is adjusted properly so the flow accelerates throughout the entire nozzle. In that case the ratio P_b/P_0 is the design pressure ratio $(P_b/P_0)_d$. For any pressure ratio below $(P_b/P_0)_d$, or above $(P_b/P_0)_d$ and below the pressure ratio of Case (b), the flow will present a non-isentropic behavior. A shock wave or a series of shock waves and expansion waves will appear in the flow, either inside the nozzle or outside in the free jet, to bring the flow pressure to the level of the back pressure P_b. This will result in an undesired subsonic flow.

The design pressure ratio $(P_b/P_0)_d$ for a shockless supersonic nozzle flow is found with the one-dimensional isentropic relation for a calorically perfect gas. Under the stated assumptions

the back pressure and the stagnation pressure are the only functions of the exit design Mach number (M_e)[4]:

$$\left(\frac{P_0}{P_b}\right)_d = \left\{1 + \left(\frac{\gamma - 1}{2}\right)M_e^2\right\}^{\frac{\gamma}{\gamma-1}} \quad \text{(Eq 1)}$$

where γ is the gas specific heat ratio C_p/C_v. If the desired exit Mach number and the back pressure are known, the required stagnation pressure is found from Eq 1.

2.3 Specific Geometry for a Shock-Free Supersonic Flow

Even if the design pressure ratio $(P_b/P_0)_d$ is used, not all convergent-divergent nozzles will produce the desired supersonic flow. The right specific nozzle geometry must be used. The design requirement from the one-dimensional isentropic flow analysis is entirely fulfilled if the design pressure ratio (Eq 1) is used with the proper throat to exit area ratio given by[4]:

$$\frac{A_e}{A^*} = \frac{1}{M_e}\left\{\left(\frac{2}{\gamma + 1}\right)\left[1 + \left(\frac{\gamma - 1}{2}\right)M_e^2\right]\right\}^{\frac{\gamma+1}{2(\gamma-1)}} \quad \text{(Eq 2)}$$

where A_e is the nozzle exit area and A^* is the nozzle throat area. If this geometric ratio is not respected, shock waves will appear in the flow, slowing it to subsonic velocities.

3. Design Mach Number Limitation Using the One-Dimensional Approach

In this section the design limitation of the nozzle exit Mach number, M_e, is presented. As in Section 2, the one-dimensional approach is used. First, the limitation due to the stagnation temperature is shown. Second, another reason for limiting the exit Mach number is presented, resulting from the shock wave-particle interactions.

3.1 Stagnation Temperature

According to Eq 1, the stagnation pressure, but not the stagnation temperature, plays a fundamental role in the process of generating a supersonic flow at a specific exit Mach number. The pressure ratio and the specific geometry (through its exit to throat area ratio, A_e/A^*) determine the exit Mach number. However, the stagnation temperature has a direct influence on the exit velocity of the fluid.[8] For a perfect gas, the speed of sound is given by $C = (kRT)^{1/2}$, where C is the speed of sound in the gas and R is the gas constant. Since the velocity of the fluid is given by the relation $v = M \times C$, the temperature plays a direct role in the exit velocity of the fluid. The higher the exit temperature of the gas is, the higher is the speed of sound at the exit. Consequently, the higher the gas exit temperature, the higher is the exit velocity of the gas for a specified exit Mach number. It is therefore possible to use a supersonic nozzle designed to operate at a specific exit Mach number and obtain different exit velocities by varying the stagnation temperature.

Knowledge of the required exit gas velocity and of the nozzle design exit Mach number determines both the exit and the stagnation gas temperatures, T_e and T_0.The exit gas temperature T_e is found by $T_e = (V/M_e)^2/(\gamma R)$, and the stagnation temperature T_0 is found with the following equation, expressing the energy conservation law[4]:

$$\frac{T_0}{T_e} = \left\{1 + \left(\frac{\gamma - 1}{2}\right)M_e^2\right\} \quad \text{(Eq 3)}$$

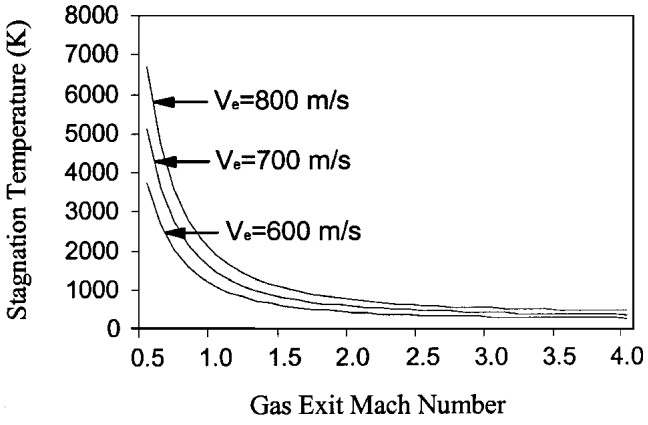

Fig. 2 Required gas stagnation temperature (T_0) as a function of the gas exit Mach number (M_e). Three exit velocities are shown: 600, 700, and 800 m/s.

Figure 2 presents the gas stagnation temperature required for different gas exit Mach numbers and velocities. The results are shown for three exit velocities: 600, 700, and 800 m/s. These velocities are representative of the velocities used in the CGDS process.[6] The results show that the required stagnation gas temperature drops with the increasing gas exit Mach number, resulting in a smaller heater needed. The solid particles injected in the jet will encounter temperatures ranging from the exit jet temperature T_e to the stagnation temperature T_0. The latter is found not only inside the tank at the stagnation section but also at the stagnation point, on the substrate, as the flow is heated during its deceleration. It is required to use low stagnation temperatures to obtain many of the benefits of the CGDS process.[1,2] Figure 2 can be used to determine the minimum nozzle exit Mach number that ensures injected particles will not be exposed to a too high gas temperature during their flight and also once they are deformed on the substrate. Setting the maximum allowable T_0 to 1000 K, based on the current practice in CGDS,[5-7] shows that the minimum exit Mach number should generally be kept above 1.5. This limit increases with the required exit velocity.

3.2 Shock Wave-Particle Interactions

The stagnation temperature is not the only factor fixing limits to the gas exit Mach number. The presence of unavoidable shock waves in the jet and their interactions with the solid particles to be accelerated and sprayed also restricts the gas exit Mach number.

3.2.1 Shock Waves. Shock waves are the result of the adjustment of a supersonic flow to downstream conditions or perturbations. They represent an abrupt change in the flow properties in which finite variation in pressure, temperature, density,

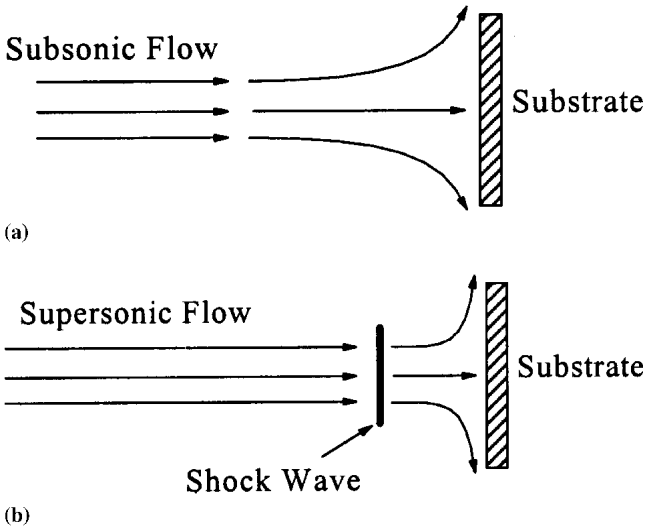

Fig. 3 **(a)** Subsonic flow impinging a substrate, no shock wave, and **(b)** supersonic flow impinging a substrate. A shock wave is present in front of the substrate for this supersonic flow.

and velocity occurs over a thickness comparable to the mean free path of the gas molecules involved.[4] In the case of a flow impacting with a substrate, the latter represents the downstream perturbation. This perturbation is transmitted through the flow by infinitesimal pressure waves, emitted at the surface of the perturbation. These pressure waves travel at the local speed of sound with respect to the flow. If the flow is subsonic, these pressure waves can travel upstream and signal to the fluid ahead the presence of the substrate. The fluid can then adjust to the presence of the perturbation with gradual changes in the flow properties, as depicted in Fig. 3(a). If the flow is supersonic, the pressure waves cannot travel upstream, so the flow is unable to sense the presence of the perturbation. An abrupt change in the flow properties occurs as it gets close to the substrate: a shock wave is formed in front of the substrate. The shock wave decelerates the flow to a subsonic velocity. This subsonic flow can now receive the pressure waves emitted from the substrate and adjust to the presence of that perturbation through gradual changes. This situation is shown in Fig. 3(b). Due to the large gradients of the flow properties occurring through the shock wave, frictional or dissipative effects are present in the flow and make it an irreversible phenomenon. The flow going through a shock wave is therefore not isentropic.

However, the flow must satisfy the mass, energy, and momentum equations throughout the shock wave; from these equations, it is possible to get the following relations,[4] linking the properties of the flow before and after the shock wave:

$$V_2 / V_1 = \rho_1 / \rho_2 \quad \text{(Eq 4)}$$

$$\rho_2 / \rho_1 = (\gamma + 1)M_1^2 / ((\gamma - 1)M_1^2 + 2) \quad \text{(Eq 5)}$$

In Eq 4 and 5, ρ is the gas mass density, γ is the specific heat ratio, M is the Mach number of the flow, V is the velocity of the flow, and subscripts 1 and 2 refer to the properties before and after the shock wave.

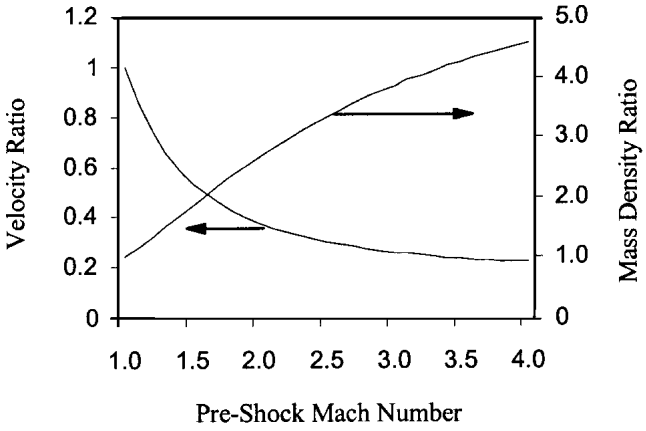

Fig. 4 Velocity ratio V_2/V_1 and mass density ratio ρ_2/ρ_1 across a normal shock wave as a function of the pre-shock Mach number (M_1)

Figure 4 shows the ratio of the mass density and of the velocity across a shock wave as functions of the Mach number of the flow before the shock wave, referred to as the pre-shock Mach number. The velocity decreases through the shock wave while the mass density increases. The larger the pre-shock Mach number, the larger the changes through the shock wave. Because the shock thickness is small compared with the characteristic length of the flow, it is treated as a local discontinuity of the gas flow properties. By itself, the discontinuity has no effect on the particles, but since the shock wave considerably changes the gas flow properties, and in particular the gas mass density and velocity, this effect will be referred to as the shock-particle interaction.

3.2.2 Shock-Particle Interaction. After the shock, the solid particles are slowed down due to the increased gas mass density and the decreased gas velocity. The drag force acting on a particle is expressed by

$$D = 0.5\rho V_{rel}|V_{rel}|SC_D \quad \text{(Eq 6)}$$

where D is the drag force exerted on the particles, ρ is the mass density of the gas, V_{rel} is the relative velocity between the solid particle and the gas, S is the projected area of the particle, and C_D is the drag coefficient, which is a function of the Mach number.

Figure 5 shows the drag parameter DP = 0.5 $\rho V_{rel}|V_{rel}|C_D$ after the shock wave as a function of the pre-shock Mach number. Two cases are shown. The first one is for particles that have attained the gas velocity before reaching the shock wave, while the second one is for the case of particles that have attained only 75% of the gas velocity. It has been found that the drag parameter DP is independent of the gas velocity before the shock wave; it is only a function of the Mach number before the shock wave. It is concluded from Fig. 5 that the higher the Mach number before the shock wave (therefore the nozzle design exit Mach number) the higher the drag on the particles after the shock wave. Even if the drag coefficient C_D reaches a maximum for a Mach number of around 1.6, it does not reflect much in the drag parameter DP since the product of the gas density and the relative velocity always increases. The use of a high Mach number is not desirable, establishing a limit on the maximum Mach number to use.

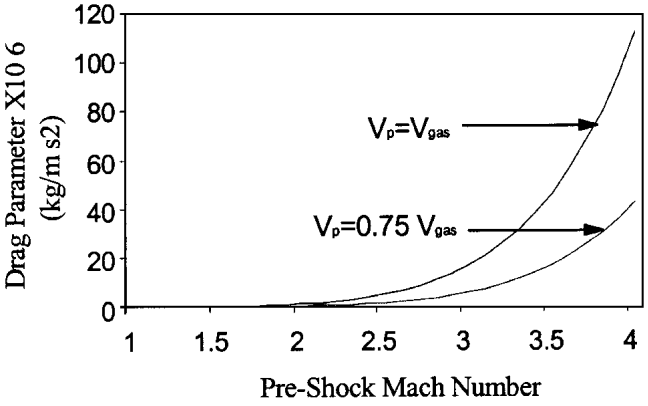

Fig. 5 Drag parameter DP, acting on the solid particle directly after the shock wave, according to the pre-shock Mach number

However, Fig. 5 is not complete by itself and cannot be used to determine the maximum allowable exit Mach number. The size and the type of the powder used are also important. From a kinematics point of view, the velocity of a particle can be tracked by the following equations:

$$X = X_0 + V_x \, dt \quad \text{(Eq 7)}$$

$$V_x = V_{x0} + D/m \, dt \quad \text{(Eq 8)}$$

and

$$\frac{D}{m} = \frac{0.5\rho|V_{rel}|V_{rel}C_D}{\frac{4}{3}r_{part}\rho_{part}} \quad \text{(Eq 9)}$$

In these equations, X is the position of the particle, X_0 is the initial particle position, V_x is the velocity of the particle, V_{x0} is the velocity of the particle before the shock wave, D is the drag force on the particle, m is the mass of the particle, dt is the time step, ρ is the gas mass density, V_{rel} is the relative velocity between the particle and the gas, C_D is the drag coefficient of the particle, r_{part} is the radius of the particle, and ρ_{part} is the mass density of the particle. The drag force will have a larger effect on the light particles, as seen from Eq 8. Equation 9 shows that the important physical parameter that will establish the response of the particles is the product $r_{part}\rho_{part}$.

This factor takes into consideration the type and the size of the particle. Particles of two different materials will experience the same trajectory and velocity if they have the same $r_{part}\rho_{part}$. Therefore, particle trajectories will be studied according to this parameter.

3.2.3 Model. To study the effect of a one-dimensional normal shock wave on the particles velocity, a simple numerical model was developed and used. The model represents an idealized situation: the flow is supersonic and one-dimensional before going through a normal shock wave and is subsonic and one-dimensional for an infinite length after the shock wave. To include the effect that the particles velocity may be different than the gas velocity before the shock wave, three particle velocities are assumed: $V_p = V_{gas}$, $V_p = 0.9\ V_{gas}$, and $V_p = 0.75\ V_{gas}$. The effect of the particles on the gas velocity is assumed to be negligible. The situation is illustrated in Fig. 6.

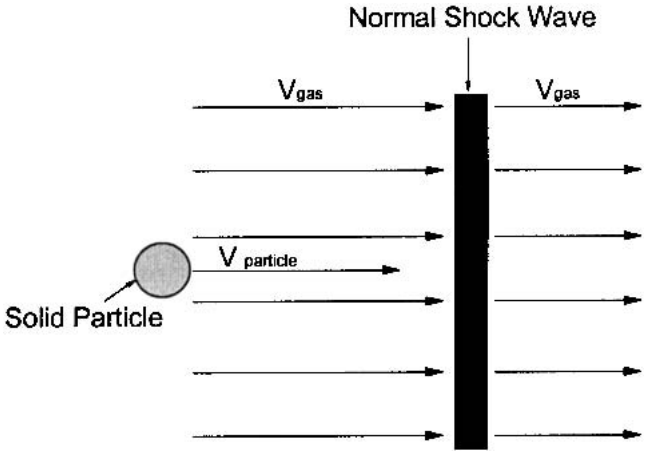

Fig. 6 One-dimensional flow through a normal shock wave

Following these assumptions, the velocity of the particles after the shock will be higher than in a real situation because the pressure and viscous forces would slow down the jet flow. Nevertheless, the results should give a good trend of the effect of the shock wave on the particles velocity.

The model uses Eq 4 and 5 to predict the flow properties after the normal shock wave, and uses Eq 7-9 to track the particles positions and velocities. Various forms of the drag coefficient were used[9-11] and all gave similar results. Four different flows with different pre-shock Mach numbers (1.7, 2, 3, and 4) were studied. For these four cases the gas velocity was fixed at 850 m/s and the pressure was set at 100 kPa. It is assumed for this study that the critical velocity is equal to the gas velocity.

3.2.4 Results. Figure 7 reports the effect of the shock wave on the velocity ratio $V/V_{critical}$ for particles having $r_{part}\rho_{part}$ equal to 80 μm · g/cm^3 with respect to the distance after the shock wave. That distance is fixed at 2 mm, a representative shock-substrate distance, and the particle velocity is assumed to be equal to the gas velocity. It shows that as the pre-shock Mach number increases, the velocity ratio of the particles decreases with a ratio of 0.86 for the case where the Mach number is 4. It also shows that the particle velocity decreases in a non-linear way with the Mach number. This reveals that the use of an exit Mach number higher than 3 could possibly lead to high velocity loss. If the distance between the shock wave and the substrate is around 2 mm, a Mach number of 3 would constitute an acceptable maximum limit without considerable velocity loss.

Figure 8 reports the same effect, for particles having $r_{part}\rho_{part}$ equal to 8 μm · g/cm^3. The effect of the shock wave is greater on those particles. Even for an exit Mach number of 2, the velocity ratio of the particles is reduced to 0.90 over that short distance and to as low as 0.44 for the case of a Mach number of 4.

Figures 9 and 10 compare the effects of the shock wave on the particles velocity for cases where the particles would not have been accelerated to the level of the pre-shock gas velocity. Two cases are presented ($V_p = 0.9\ V_{gas}$ and $V_p = 0.75\ V_{gas}$) along with the case where the particles have been accelerated to the velocity of the gas. The flow Mach number is set to 3. The results show

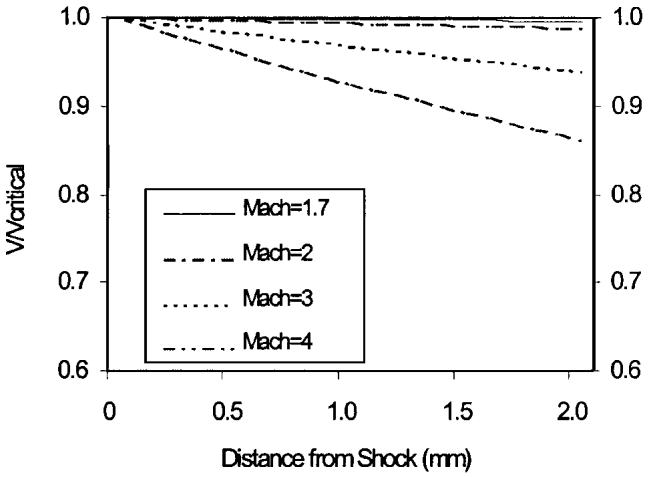

Fig. 7 Velocity ratio after the shock wave for particles with $r_{part}\rho_{part}$ equal to 80 μm · g/cm^3. Four pre-shock Mach numbers are shown: 1.7, 2, 3 and 4.

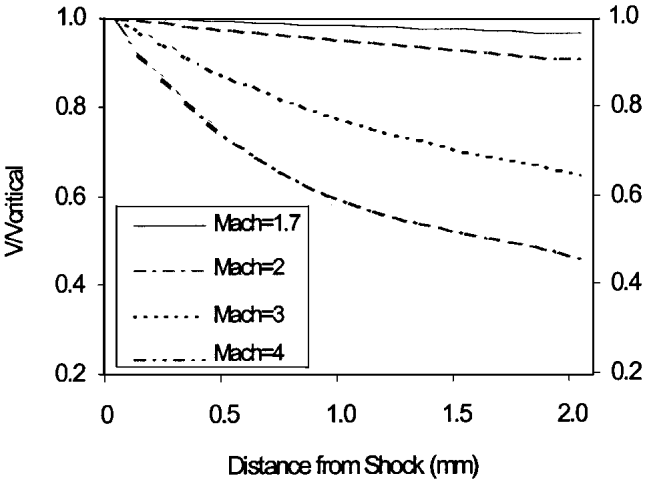

Fig. 8 Velocity ratio after the shock wave for particles with $r_{part}\rho_{part}$ equal to 8 μm · g/cm^3. Four pre-shock Mach numbers are shown: 1.7, 2, 3 and 4.

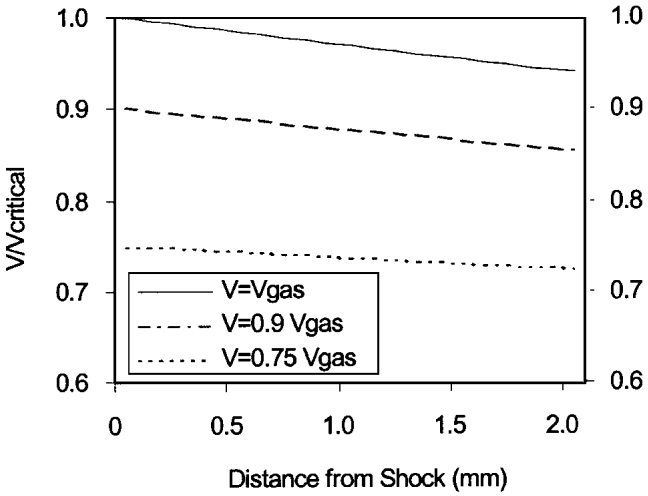

Fig. 9 Velocity ratio after the shock wave for particles with $r_{part}\rho_{part}$ equal to 80 μm · g/cm^3. The gas Mach number is set at 3. Velocity of the particle before the shock is V_{gas}, 0.9 V_{gas}, and 0.75 V_{gas}.

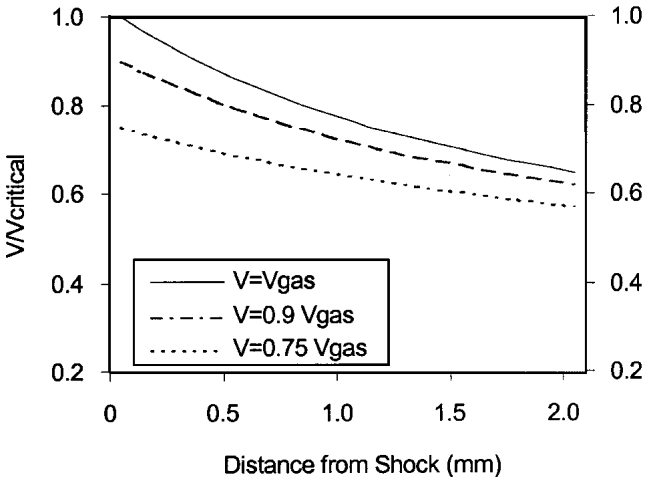

Fig. 10 Velocity ratio after the shock wave for particles with $r_{part}\rho_{part}$ equal to 8 μm · g/cm^3. The flow Mach number is set at 3. Velocity of the particle before the shock is V_{gas}, 0.9 V_{gas} and 0.75 V_{gas}.

that the slowing effect of the shock wave on the particles is reduced, as the difference between the gas and particles velocities increases, but not significantly enough to neglect it for small values of $r_{part}\rho_{part}$.

From these results, it is concluded that the CGDS process is experiencing the same problem as classic supersonic aerodynamics[4]; one has to find a way of slowing down the gas without loss, after any device has once accelerated it. It is thus good aerodynamic practice to avoid accelerating the gas more than is necessary.

This gives the upper limit of the Mach number that one should use in cold spray. The minimum was fixed around 1.5 for thermal consideration and the upper limit is imposed by the slowing effect of the shock wave around 3.

So far, the simple one-dimensional isentropic flow has been used to come up with these conclusions. The next part of the paper will verify if these trends remain when a two-dimensional axisymmetric system is studied. A numerical model will be used and verified with experimental data.

4. Experimental Procedures

To validate the numerical model used for the flow field prediction, two sets of experimental measurements are conducted. Since the pressure is the fundamental parameter controlling the flow inside the nozzle, the first set of measurements conducted is the static pressure measurements along the CGDS nozzle length. These measurements allow establishment of the quality of the prediction of the model for both cases: with and without the presence of shock waves inside the nozzle. The second set of measurements conducted is the measurement of the pressure distribution on the substrate. These measurements should assess the quality of the model for the jet and through the shock wave located in front of the substrate.

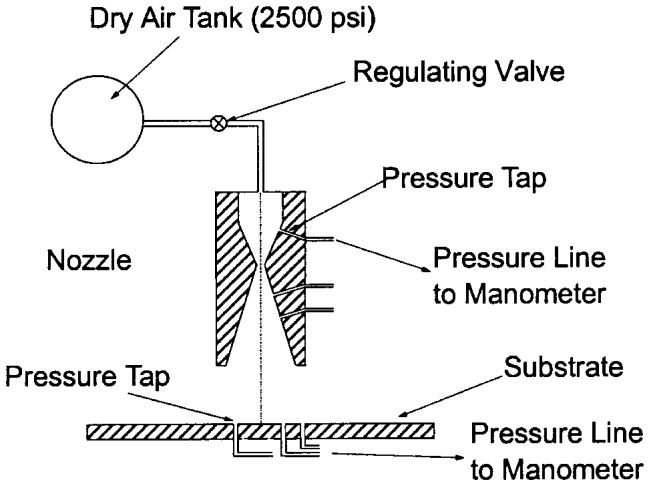

(a)

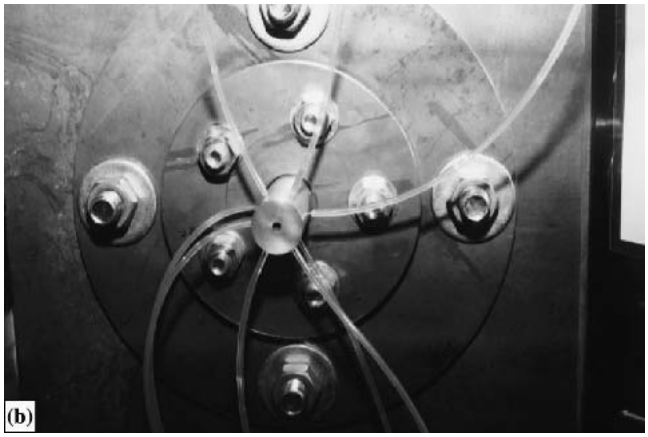

Fig. 11 **(a)** Cold gas dynamic spray gun system, not to scale; **(b)** photograph of the nozzle and pressure lines

4.1 Nozzle Flow Measurements

Figure 11 shows the experimental CGDS setup used for this work. The convergent-divergent nozzle is made of brass. It is axisymmetric, with a throat diameter of 2 mm and an exit diameter of 2.48 mm. The distance between the throat and the exit plane is 20 mm, and the nozzle expands linearly for manufacturing simplicity. The exit design Mach number of the nozzle flow is M_e = 1.7. To monitor the flow inside the nozzle, nine static pressure taps were drilled according to established criteria.[12]

The pressure taps are distributed over the length and circumference of the nozzle. They are concentrated in the throat region and in the diverging section. This distribution is required since the pressure gradients are higher in the former region, while shock waves that may be present in the diverging section of the nozzle would induce large pressure gradients in the latter zone. The pressure taps are located 3 mm apart from each other, with a 60° angle between them. Each tap is connected to a digital manometer. The working gas used in this work is air. The high-pressure air is delivered to the inlet of the nozzle from two compressed air tanks after going through a regulating valve that sets the pressure to the required stagnation pressure. For the simplicity of the setup and to limit the number of parameters to control, the gas is not heated by heaters before going through the nozzle. Instead, the gas is naturally brought to the ambient temperature of 22 °C by allowing it to travel in a copper pipe long enough to ensure the temperature.

A first set of measurements is done for the case of normal operating conditions where no shock waves are present inside the nozzle. The stagnation pressure is set at the regulating valve to 493 kPa, and measurements of the pressure inside the nozzle are made. A second set of measurements is conducted for the off-design case where a normal shock wave is present inside the nozzle. To get that flow, a stagnation pressure of 145 kPa is used.

4.2 Substrate Flow Measurements

The substrate used in this work is a 15 cm diameter round brass plate. It can be moved to vary the standoff distance. The center of the substrate is aligned with the nozzle axis. To monitor the flow at the surface of the substrate, 29 pressure taps are distributed over the radius. Twelve of the 29 pressure taps are located within the first 3.5 mm radius of the substrate. Each pressure tap is connected to a digital manometer. Measurements are made at a standoff distance of 10 mm for a stagnation pressure of 493 kPa. The results of the test cases are presented in the next section, with the predicted values of the two-dimensional axisymmetric model.

5. Numerical Model and Validation

In this section, the numerical model used to predict the gas flow characteristics inside the convergent-divergent nozzle and in the impinging supersonic jet is presented. The equations governing the gas flow under study are stated, along with their classification type. The choice of a flow solver, based on its accuracy and performances, is then presented. The operating and boundary conditions used in this work follow. Finally, the three validation test cases are presented and the experimental measurements are compared with the model predictions to assess the quality of the model.

5.1 Governing Equations

The equations governing the steady-state CGDS flow are the mass, momentum, and energy conservation equations. Due to the transonic nature of the flow under study, this set of equations is classified as elliptic in the subsonic part of the flow, parabolic in the sonic part of the flow, and hyperbolic in the supersonic part of the flow. This difference in the classification type of the equations is the result of the way the perturbations are transmitted in the flow. To properly represent the physical system, the numerical discretization scheme must reproduce this physical feature. This feature increases the level of complexity involved in solving the governing equations since the numerical discretization scheme used to solve each type of equation set is different. To account for turbulence in the flow, a k-ε turbulence model is used. The flow being compressible, the gas mass density is not constant, and one more equation is used to close the system of equation: the perfect gas law.

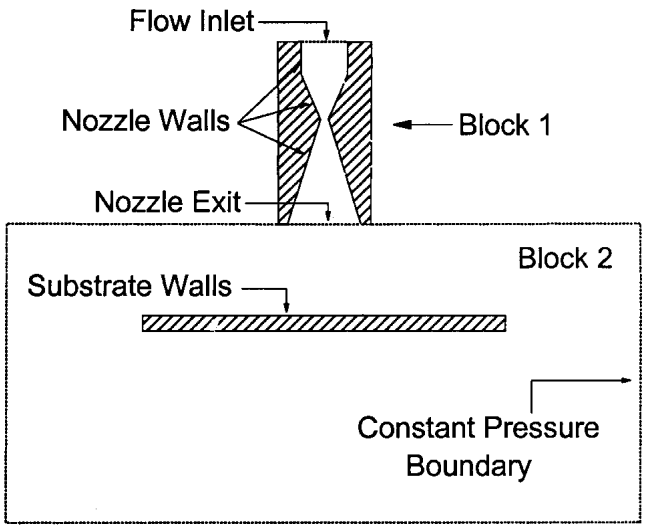

Fig. 12 Schematic representation of the calculation domain and boundaries. The domain is divided in two blocks. Block 1 is the nozzle flow, and Block 2 is the impinging jet flow.

5.2 Flow Solver

Before carrying out the computational solution of the three test cases, two flow solvers are used and their performances are compared. The first flow solver used is a finite-difference flow solver developed and validated for the supersonic direct current (dc) plasma spray torch.[13] The second one is the commercial finite-volume flow solver, Fluent (FLUENT, Inc., Lebanon, NH). The advantage of the first solver over the second one is that it allows control of the artificial viscosity used to stabilize the solution. Artificial viscosity can become large enough to alter the solution of a transonic flow, therefore its control is important. Artificial viscosity should be limited to the minimum value required to stabilize the solution. The solutions of a transonic nozzle flow obtained from the two solvers were compared, and no significant differences were observed between the two solutions. Performance comparison (CPU time) between the two solvers revealed that the Fluent flow solver is 30% faster in solving the flow. It was therefore decided that the Fluent flow solver would be used, the effect of the artificial viscosity introduced being small. The method used to solve the flow field is a coupled-implicit method and the discretization scheme used is a second-order scheme.

5.3 Operating and Boundary Conditions

The computational domain and the boundary conditions used to predict the gas flow characteristics for the three test cases are shown in Fig. 12. It was found that the convergence rate of the numerical model is higher when the computational domain is divided into two blocks, so this approach is used. The nozzle forms the first block, and the region where the supersonic jet impinges the substrate forms the second block. The operating and boundary conditions used are now presented for each test case.

5.3.1 Test Case One: Shockless Nozzle Flow. The operating conditions for the shockless nozzle flow test case are as follows. The stagnation pressure and the stagnation temperature are, respectively, 493 kPa and 22 °C. The exhaust back pressure is fixed by the atmospheric pressure at 100 kPa.

Accordingly, the boundary conditions for Block 1 are set as follows. At the nozzle inlet the flow is subsonic. The stagnation pressure and temperature are fixed at the operating values. At the exit of the nozzle, the flow is supersonic. No information can travel upstream. Therefore, all the flow variables are extrapolated from the inside solution of the nozzle flow. At the nozzle walls, the non-slip condition is used and adiabatic walls are assumed. The latter condition is not respected in reality. However, it was found that this approximation, compared with a fixed wall temperature, does not influence significantly the solution of the flow field. Since the nozzle wall temperature is usually unknown, the adiabatic wall assumption is used. The flow in Block 2 is not solved for this test case.

5.3.2 Test Case Two: Nozzle Flow With the Presence of a Shock Wave. The operating conditions for this test case are as follows. The stagnation pressure and the stagnation temperature are, respectively, 145 kPa and 22 °C. The exhaust back pressure is fixed by the atmospheric pressure at 100 kPa.

The boundary conditions used for this test case are as follows. At the nozzle inlet, the stagnation pressure and temperature are fixed at 145 kPa and 22 °C respectively. The non-slip and adiabatic conditions are used at the nozzle walls. With the presence of a shock wave inside the nozzle, the flow decelerates to subsonic speed and information can travel upstream from the nozzle exit. The pressure is therefore fixed at the exit plane of the nozzle to the back pressure of 100 kPa. As for Test Case One, the flow in Block 2 is not solved.

5.3.3 Test Case Three: Supersonic Jet Impinging the Substrate. The operating conditions used for this test case are the same as those used in the first test case. The substrate standoff distance is set at 10 mm from the exit of the nozzle.

The solutions of the flow at the nozzle exit of the first test case are used as boundary conditions for the free supersonic jet. The pressure at the constant pressure boundary is set at 100 kPa. The no-slip velocity condition is used at the substrate surfaces and these surfaces are assumed to be at a uniform and constant temperature of 22 °C.

5.4 Validation

Comparisons between the measured pressure distribution and the numerical prediction are illustrated in Fig. 13. It is concluded that the model predicts accurately the shockless supersonic nozzle flow. Figure 14 illustrates the measured pressure distribution and the numerical model prediction when a normal shock wave is present inside the nozzle (Test Case 2). It shows that the numerical model properly predicts the flow and the shock wave position and strength. Figure 15 shows the pressure distribution measured on the substrate and the prediction of the numerical model for Test Case Three.

Once again, the agreement is good. The differences between the model prediction and the measurements are attributed to two factors. First, it is difficult to position the substrate exactly at the nozzle axis. Therefore, some positioning errors are introduced. Second, the k-ε model used may not be the best-suited turbulence model for this kind of flow. The presence of the shock wave should not be considered as a cause for the discrepancy between the model and the measurements since the two previous test cases showed that the model could accurately predict supersonic flow with and without the presence of a shock wave. Ac-

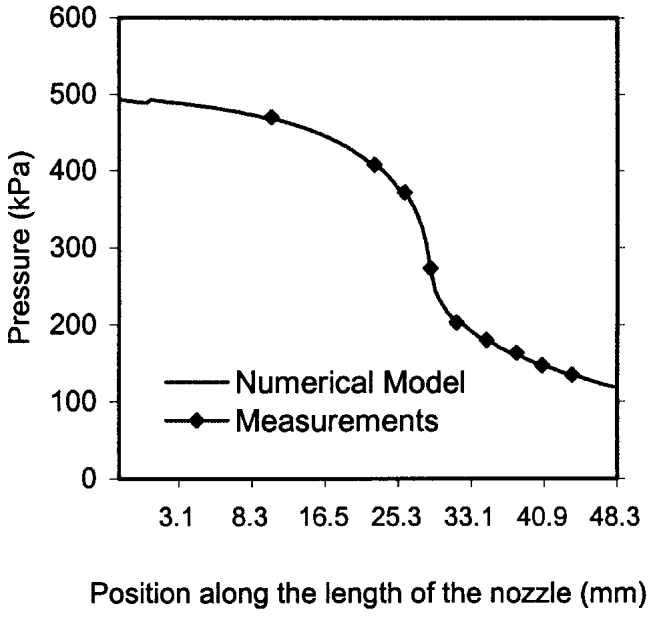

Fig. 13 Comparison between the numerical prediction and the measurements for the shockless supersonic (Mach = 1.7) nozzle flow; pressure distribution at the nozzle wall

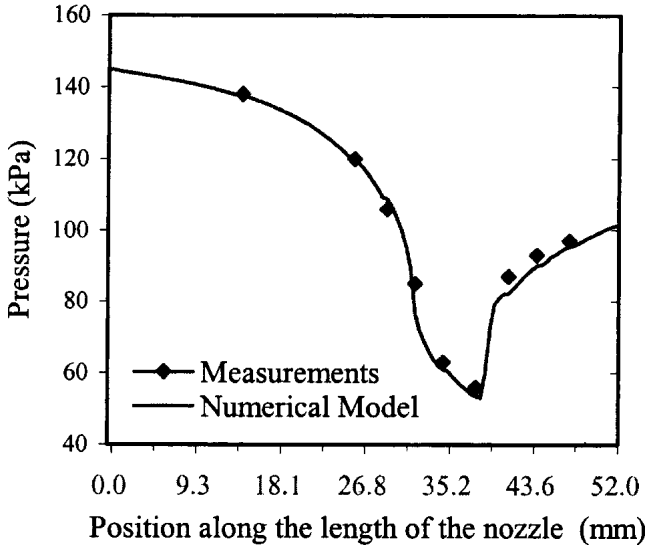

Fig. 14 Comparison between the numerical prediction and the measurements for the nozzle flow with a shock wave inside the nozzle; pressure distribution at the nozzle wall

cording to the three validation test cases done, it is concluded that the numerical model predicts the flow accurately.

6. Design Mach Number Limitation Using the Two-Dimensional Flow Model

In this section the design limitation of the nozzle exit Mach number is presented, using the results of the two-dimensional

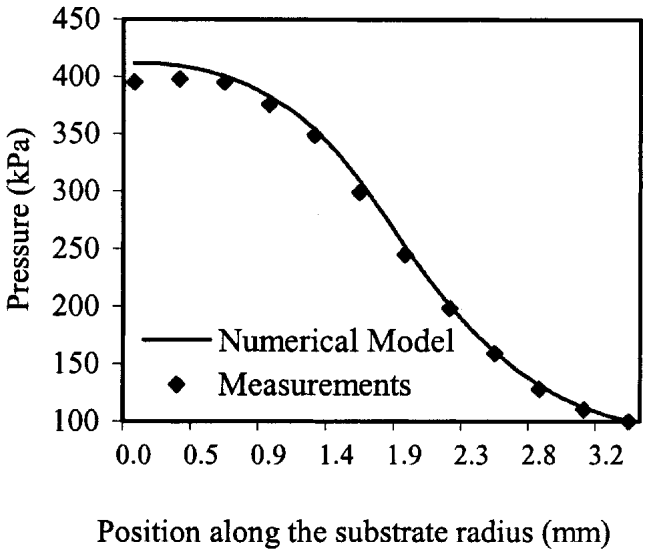

Fig. 15 Comparison between the numerical prediction and the measurements for the supersonic flow (Mach = 1.7) over the substrate; pressure distribution at the substrate wall

flow model validated in the previous section. First, the limitation due to the stagnation temperature is shown. Then the limitation due to the shock wave-particle interactions is presented. The nozzle exit velocity is set at 850 m/s.

6.1 Stagnation temperature

The particles injected in the jet, as mentioned previously, will be exposed to temperatures ranging from the nozzle exit temperature (the coldest temperature in the flow) to the stagnation temperature. The latter is experienced by the particles near the stagnation point on the substrate. In the one-dimensional flow approach, it was assumed that the flow is adiabatic, and therefore the stagnation temperature before and after the shock wave is constant. However, in reality, there is a possible heat transfer between the jet and the ambient air. This heat transfer could lead to a different stagnation temperature after the shock wave to which the particles would be exposed in the vicinity of the substrate. It is therefore necessary to check if this heat transfer significantly affects the stagnation temperature after the shock wave.

Figure 16 shows the temperature contours of the $M_e = 1.7$ impinging jet. The standoff distance is set at 10 mm and the required stagnation temperature before the nozzle was set at 961 K. There is a shock wave located in front of the substrate reducing the flow from supersonic to subsonic level. As can be seen, the stagnation temperature after the shock wave is not affected significantly and remains nearly constant. It is therefore a good approximation to assume that the stagnation temperature is constant throughout the cold spray flow. From this it can be concluded that even if the particles are not injected in the flow from the stagnation section, the particles will be exposed to the stagnation temperature once they reach the substrate. As concluded with the one-dimensional flow model, it is a good practice to limit the minimum exit Mach number to avoid the need to use too high stagnation temperatures.

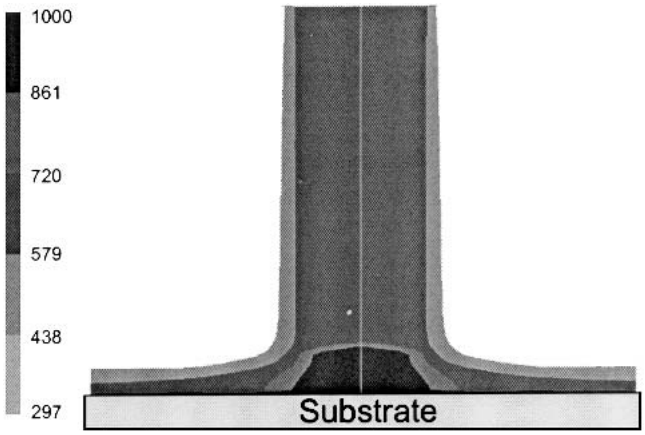

Fig. 16 Temperature field for the Mach = 1.7 jet. Stand-off distance is 10 mm. A shock wave is present in front of the substrate. Temperatures are in Kelvin.

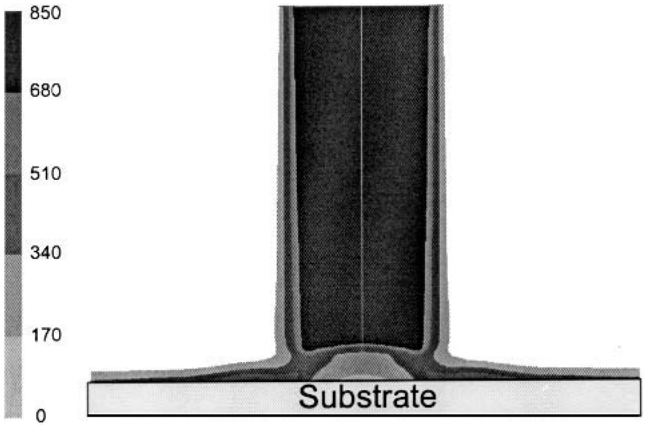

Fig. 17 Velocity field for the Mach = 1.7 jet. Stand-off distance is 10 mm. A shock wave is present in front of the substrate. Velocities are in m/s.

6.2 Shock Wave-Particle Interactions

The presence of a shock wave in the jet and its interaction with the solid particles to be accelerated and sprayed is now presented.

Figure 17 shows the velocity magnitude of the M_e = 1.7 impinging jet. The standoff distance is set at 10 mm. The high velocity core is preserved throughout the length up to the shock wave. Entrainment of ambient air is seen as a shear layer is developing along the jet.

Figure 18 presents the velocity of the gas along the axis of the jet, for the same case of M_e = 1.7. It shows that the velocity decreases sharply through the shock wave from 850-420 m/s. This decrease follows well the prediction of Eq 4, which is 390 m/s. Equation 4 is therefore useful to predict the post-shock velocity even in the case of an axisymmetric flow. The shock wave is located approximately at 1.45 mm before the substrate. After the velocity drop caused by the shock wave, the flow velocity is further reduced to meet the stagnation condition at the flat plate surface.

Using the velocity distribution along the axis predicted by the two-dimensional turbulent flow model, the one-dimensional particle model used in Section 3 is now used to predict the particles position and velocity along the axis. It is assumed that the particles were injected upstream in the nozzle, directly at the axis of the nozzle. The particles velocity is assumed to be equal to the gas velocity before the shock. Four different supersonic flows were studied with different pre-shock Mach numbers: 1.7, 2, 3, and 4. The exit gas velocity and pressure are set constant at 850 m/s and 100 kPa.

Figure 19 reports the effects of the shock wave on the velocity ratio $V/V_{critical}$ for particles having $r_{part}\rho_{part}$ equal to 80 μm · g/cm^3 with respect to the distance after the shock wave. It is seen that the distance between the shock wave and the substrate decreases with the gas exit Mach number from 1.95 mm (for M_e = 1.7) to 1.15 mm (for M_e = 4). It shows that as the pre-shock Mach number increases, the velocity ratio of the particles at the substrate decreases with a ratio of 0.88 for the case where M_e = 4. These results are close to those obtained previously using the one-dimensional approach for the flow. Even though the gas velocity decreases to zero in the two-dimensional case, the particles with a large $r_{part}\rho_{part}$ have enough momentum to overcome the increased drag over the short shock-substrate distance but are still affected by the large resulting drag. Again, as found by using the one-dimensional flow approach, this reveals that the use of a high exit Mach number should be avoided due to the resulting velocity loss.

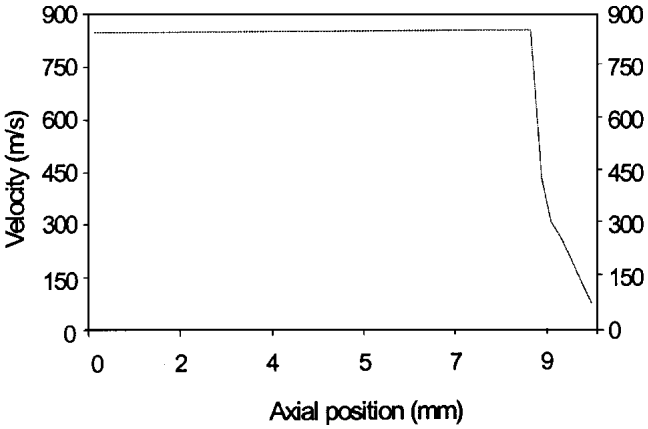

Fig. 18 Gas velocity along the axis of the Mach = 1.7 jet. The sharp reduction of the velocity caused by the shock wave is shown.

Figure 20 reports the same effect, for particles having $r_{part}\rho_{part}$ equal to 8 μm · g/cm^3. The effect of the shock wave is greater on those particles. Even for an exit Mach number of 1.7, the velocity ratio of the particles at the substrate surface is reduced to 0.90 over the short shock-substrate distance and to as low as 0.40 for the case of an exit Mach number of 4. In that case, the results are considerably different than those obtained using the one-dimensional flow approach.

Figure 21 presents the ratio $V/V_{critical}$ as a function of $r_{part}\rho_{part}$ for various gas Mach numbers. Again, $V_{critical}$ is set to 850 m/s and the particle velocity is assumed to be equal to the gas velocity before the shock wave. It is seen that when cold spraying small/light particles, the Mach number used has a large influence on the impact velocity of the particles. The larger the pre-

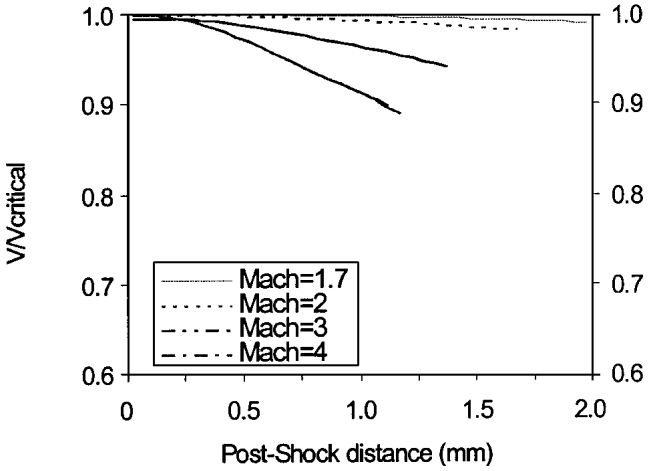

Fig. 19 Velocity ratio after the shock wave for particles with $r_{part}\rho_{part}$ equal to 80 μm · g/cm^3, based on the two-dimensional flow field. Four pre-shock Mach numbers are shown: 1.7, 2, 3, and 4.

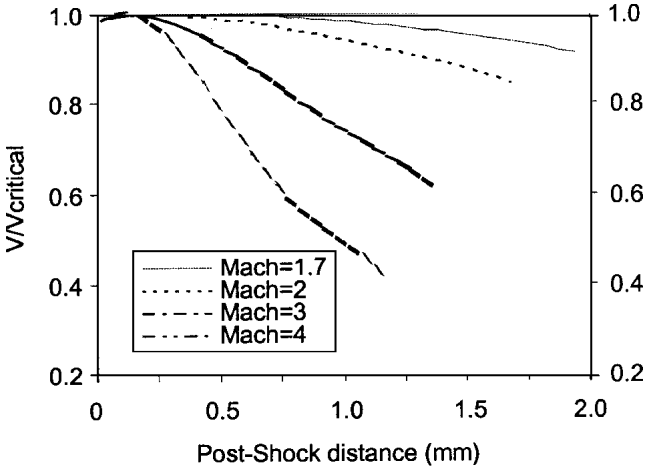

Fig. 20 Velocity ratio after the shock wave for particles with $r_{part}\rho_{part}$ equal to 8 μm · g/cm^3, based on the two-dimensional flow field. Four pre-shock Mach numbers are shown: 1.7, 2, 3, and 4.

shock Mach number, the larger the effect or the strength of the shock wave in front of the substrate. It would therefore be a good practice to limit the design Mach number of the cold spray jet to avoid the appearance of strong shock waves in the flow. Even particles with a large $r_{part}\rho_{part}$ parameter would benefit from this practice.

7. Conclusion

In the design phase of a cold spray nozzle, the only fixed parameter is the velocity to which the solid particles to be sprayed must be accelerated before impacting on the substrate. This, in turn, fixes the minimum gas exit velocity to use. To achieve this exit jet velocity, different nozzles may be used according to their design exit Mach number fixed by the geometry of the nozzle.

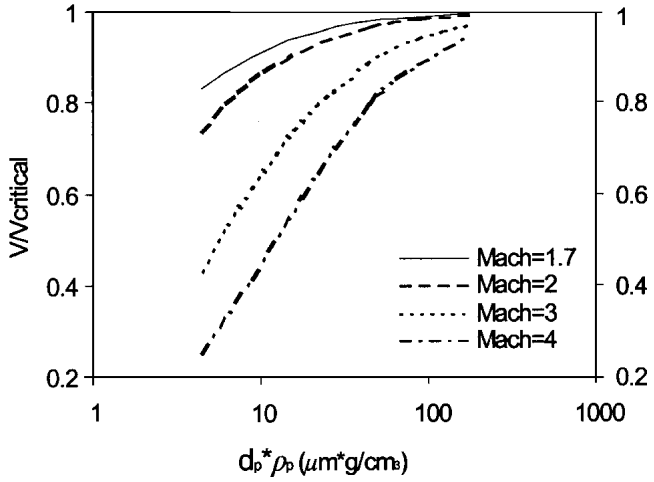

Fig. 21 Velocity ratio after the shock wave for particles with $r_{part}\rho_{part}$ based on the two-dimensional flow field. Four pre-shock Mach numbers are shown: 1.7, 2, 3, and 4.

Nozzles with a low design Mach number will require a higher stagnation temperature to produce the required velocity. This may lead to temperatures in the vicinity of the substrate that are high enough to reduce the benefits of the cold spray process since the substrate will be exposed to these temperatures. Two analyses were performed. The first one was a one-dimensional flow analysis, and the second one was a two-dimensional axisymmetric analysis using a validated numerical solver. They both showed that for the range of velocity used in cold spray the design Mach number of an air nozzle should be limited to 1.5 and above to avoid too high temperatures in the vicinity of the substrate.

Another factor also limits the range of the Mach number that should be used: the shock-particle interactions. Both analyses showed that for large/heavy particles ($r_{part}\rho_{part}$ > 200 μm · g/cm^3), the shock wave has a limited but noticeable effect on the impact velocity. This effect increases with the Mach number and becomes important at a Mach number around 3. For small/light particles ($r_{part}\rho_{part}$ < 50 μm · g/cm^3), the effect of the shock-particle interactions is very strong, even at short standoff distance and at a Mach number as low as 2. It was shown that the one-dimensional analysis underestimated that effect and may not be suitable for the shock-particle interaction study. It was found that the use of a high Mach number in the presence of small and/or light particles could significantly reduce the efficiency of the process.

It is concluded from the theoretical work done that the design Mach number of an air cold spray nozzle should be fixed according to the type and size of the particles to be sprayed, with special attention if the particles are light and/or small. More comparison with experimental data should be done to completely justify the limitation imposed on the Mach number.

Acknowledgments

The author wishes to acknowledge the financial support of the National Sciences and engineering Research Council of Canada

References

1. A.P. Alkhimov, A.N. Papyrin, V.F. Dosarev, N.I. Nesterovich, and M.M. Shuspanov: U.S. Patent 5 302 414, 1994.
2. A.O. Tokarev: "Structure of Aluminum Powder Coatings Prepared by Cold Gas-Dynamic Spraying," *Met. Sci. Heat Treat*., 1996, *38* (3-4), pp. 136-39.
3. A.P. Alkhimov, V.F. Kosarev, and A.N. Papyrin: "A Method of Cold Gas Dynamic Deposition," *Dokl. Akad. Nauk SSSR*, 1990, *315*(5), pp. 1062-65.
4. A.H. Shapiro, *The Dynamics and Thermodynamics of Compressible Fluid Flow*, Ronald Press, New York, 1953.
5. R.C. Dykhuizen and M.F. Smith: "Gas Dynamic Principles of Cold Spray," *J. Therm. Spray Technol*., 1998, *7*(2), pp. 205-12.
6. D.L. Gilmore, R.C. Dykhuizen, R.A. Neiser, T.J. Roemer, and M.F. Smith: "Particle Velocity and Deposition Efficiency in the Cold Spray Process," *J. Therm. Spray Technol*., 1999, *8*(4), pp. 576-82.
7. V. Shukla, G.S. Elliott, and B.H. Kear: "Nanopowder Deposition by Supersonic Rectangular Jet Impingement," *J. Therm. Spray Technol*., 2000, *9*(3), pp. 394-98.
8. J. Karthikeyan, C.M. Kay, J. Lindeman, R.S. Lima, and C.C. Berndt: "Cold Spray Processing of Titanium Powder" in *Proceedings of the First International Thermal Spray Conference*, C.C. Berndt, ed., ASM International, Materials Park, OH, 2000, pp. 255-62.
9. R.N. Cox and L.F. Crabtree: *Elements of Hypersonic Aerodynamics*, Academic, New York, 1965.
10. J.K. Vennard and R.L. Street: *Elementary Fluid Mechanics*, Wiley, New York, 1982.
11. C.B. Henderson: "Drag Coefficients of Spheres in Continuum and Rarefied Flows," *AIAA J.*, 1976, *14*, pp. 707-08.
12. R.P. Benedict: *Fundamentals of Temperature, Pressure and Flow Measurements*, Wiley, New York, 1984, pp. 339-73.
13. B. Jodoin, P. Proulx, and Y. Mercadier: "Numerical Study of Supersonic Direct Current Plasma Nozzle Flow," *AIAA J.*, 1998, *36*(4), pp. 578-84.